Power-Law Temperature Dependence of the Penetration Depth in a Topological Superconductor Due to Surface States

Tsz Chun Wu, Hridis K. Pal, Pavan Hosur, and Matthew S. Foster

Power-law Temperature Dependence of the Penetration Depth in a Topological Superconductor due to Surface States

Tsz Chun Wu,[1] Hridis K. Pal,[2] Pavan Hosur,[3] and Matthew S. Foster[1, 4]

[1]*Department of Physics and Astronomy, Rice University, Houston, Texas 77005, USA*
[2]*Department of Physics, Indian Institute of Technology Bombay, Powai, Mumbai 400076, India*
[3]*Texas Center for Superconductivity and Department of Physics,*
University of Houston, Houston, Texas 77204, USA
[4]*Rice Center for Quantum Materials, Rice University, Houston, Texas 77005, USA*
(Dated: October 11, 2019)

We study the temperature dependence of the magnetic penetration depth in a 3D topological superconductor (TSC), incorporating the paramagnetic current due to the surface states. A TSC is predicted to host a gapless 2D surface Majorana fluid. In addition to the bulk-dominated London response, we identify a T^3 power-law-in-temperature contribution from the surface, valid in the low-temperature limit. Our system is fully gapped in the bulk, and should be compared to bulk nodal superconductivity, which also exhibits power-law behavior. Power-law temperature dependence of the penetration depth can be one indicator of topological superconductivity.

A decade after the widespread infiltration of topology into quantum materials research, the search for electronically correlated topological phases beyond the fractional quantum Hall effect remains an urgent, but still largely unfulfilled quest. Topological superconductivity [1, 2] is sought as a platform for Majorana fermion zero modes [3] and topological quantum computation [4]. Majorana fermions could be detected by various means, including tunneling spectroscopy [5–9], the Josephson effect [5, 10, 11], as well as spin and optical responses [12, 13].

Only a handful of materials have emerged as bulk topological superconductor (TSC) candidates. Topological superconductivity has long been suspected in Sr_2RuO_4, although a consensus on chiral p-wave order is yet to be reached [2, 14–16]. Time-reversal invariant TSCs could serve as solid-state analogs of the topological superfluid phase in liquid helium (^{3}He-B) [17–23]. In the absence of a magnetic field, the predicted hallmark of such a bulk TSC is a gapless, two-dimensional (2D) Majorana fermion surface fluid. It has been argued that the odd-parity "$\hat{s} \cdot \mathbf{k}$" pairing of ^{3}He-B [24, 25] could naturally arise in doped Dirac semimetals or topological insulators [26–28]; here $\hat{s}$ and $\mathbf{k}$ respectively denote the spin-operator and momentum vectors. Alternately, doped Weyl semimetals have been shown to be natural platforms for topological superconductivity [29].

There is now substantial experimental evidence for nematicity in the superconducting doped topological insulators $(Cu,Nb)_xBi_2Se_3$ [30–33] (see also [34]), possibly indicative of odd-parity pairing. However, gapless Majorana fermions have not been conclusively detected [33, 35–37]. Recently, signatures consistent with topological superconductivity were also found in doped β-$PdBi_2$, but a conclusive detection remains elusive [38]. In $Cu_xBi_2Se_3$, only a small percentage of the exposed crystal surface was found to exhibit signatures of superconductivity in STM [33], highlighting the possibility that in inhomogeneous TSCs, there is no guarantee that Ma-

jorana fermions will appear at the *physical* surface of the sample.

It is therefore natural to seek global probes of topological superconductivity. Meissner effect penetration depth measurements in $Nb_xBi_2Se_3$ [39, 40] and in the half-Heusler compounds YPtBi [41], YPdBi and TbPdBi [42] exhibit power-law temperature suppression, which is interpreted as evidence for non-s-wave, bulk nodal superconductivity [43]. In the case of $Nb_xBi_2Se_3$, the results were interpreted as indicative of nodal odd-parity bulk pairing [39, 40], while the YPtBi results were attributed to either an exotic nodal-line "septet" pairing scenario [41, 44], or $d + id$ bulk Weyl superconductivity [44], smeared by disorder [45].

In this Letter, we show that power-law temperature (T) dependence of the penetration depth $\lambda(T)$ can arise at arbitrarily low T in a TSC with a fully gapped bulk, due to the paramagnetic response of the gapless Majorana surface fluid. This requires a nontrivial calculation employing a TSC model with a physical surface-vacuum
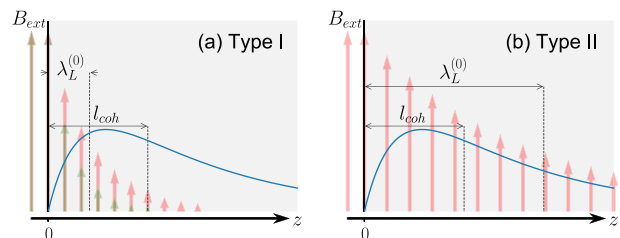

FIG. 1: Schematic illustration for (a) type I and (b) type II topological superconductors (TSCs) in an external magnetic field. The gray and white regions represent respectively the TSC and the vacuum. The red (green) arrows indicate the magnetic field that decays into the superconductor with (without) the correction due to the surface states. The scale $\lambda_L^{(0)}$ is the London (bulk-dominated diamagnetic) penetration depth. The blue line is a sketch of the Majorana surface fluid density, characterized by the coherence length l_{coh}.

boundary, and the result involves the convolution of the surface paramagnetic and bulk-dominated diamagnetic responses. It cannot be obtained from the surface Hamiltonian alone. Thus, the observation of non-exponential behavior in $\lambda(T)$ does not necessarily indicate bulk nodal pairing, and can be one diagnostic for screening possible TSCs. We also show that the magnetic field in a fully gapped TSC is sensitive to the spatial profile of the surface states. This can be used to differentiate gapless states from the surface versus those from the bulk. By contrast, STM is sensitive only to the sample surface density of states, while the finite energy resolution of ARPES might prevent the direct detection of Majorana fermions in a low-temperature superconductor. While power-law temperature dependence in the penetration depth can arise from multiple mechanisms [46, 47], it can serve as one possible indicator for bulk topological superconductivity. In general, one wants as many independent tests as possible in order to identify TSCs.

We consider "minimal" TSCs in class DIII with winding number $\nu = 1$, possessing a single surface Majorana cone. We show that the leading correction to the London response due to the presence of Majorana surface states scales as T^3. The same temperature dependence is predicted to arise in the suppression of the mass flow of superfluid ^{3}He-B through a channel, due to surface currents [48]. We calculate explicitly the magnetic field profile inside the slab, which incorporates new features introduced by the surface states. For type I TSCs, the field penetrates much deeper than the London depth into the bulk, with the scale set by the coherence length. For type II TSCs the field is modulated in a shallow region near the surface, and then decays at deeper depths according to the London length, but with an enhanced field amplitude.

Model.—We consider a superconducting slab filling up the $z > 0$ half-space, with an external magnetic field $\mathbf{B}_{\text{ext}} = B_0\,\hat{y}$ as shown in Fig. 1. We assume the field is weak enough such that $B_0 < B_{c_1}$ where B_{c_1} is the lower critical field of a type II superconductor. Under this assumption, the effect of vortex formation can be neglected and a linear response treatment is valid. The total current $\mathbf{J}$ and the vector potential $\mathbf{A}$ satisfy the static Maxwell's equation

$$\boldsymbol{\nabla}^2 \mathbf{A}(z) = -\frac{4\pi}{c}\mathbf{J}(z), \tag{1}$$

where $\mathbf{A}(z) = A(z)\,\hat{x}$, $\mathbf{B}(z) = \partial_z A(z)\,\hat{y}$, $\mathbf{J}(z) = J(z)\,\hat{x}$, and

$$\mathbf{J}(z) = \mathbf{J}_{\text{ext}}(z) - \frac{1}{c}\int_0^\infty dz'\,\Pi(z,z')\,\mathbf{A}(z'). \tag{2}$$

Here, $\mathbf{J}_{\text{ext}}(z)$ is a fictitious current generating the external magnetic field, and $\Pi(z,z')$ is the current-current correlation function capturing the linear response of the TSC.

The above equations can be expressed as

$$-2B_0 = \left[q_z^2 + \left(\lambda_L^{(0)}\right)^{-2}\right]\tilde{A}(q_z)$$
$$+ \frac{4\pi}{c^2}\int\frac{dQ_z}{2\pi}\,\tilde{\Pi}_{1,R}^{xx}(0,0,0;q_z,-Q_z)\,\tilde{A}(Q_z), \tag{3}$$

where $\lambda_L^{(0)}$ is the London penetration depth and

$$\tilde{\Pi}_{1,R}^{xx}(\Omega = 0, q_x = 0, q_y = 0; q_z, -Q_z)$$
$$= -i\int dt\,dx\,dy\int_0^\infty dz_1 dz_2\,\mathrm{e}^{-iq_z z_1 + iQ_z z_2}$$
$$\times\langle[J_1^x(t,x,y,z_1), J_1^x(0,0,0,z_2)]\rangle\,\theta(t) \tag{4}$$

is the retarded paramagnetic current-current correlation function. Here, $J_1^x(t,x,y,z)$ is the paramagnetic current flowing along the x direction and $\theta(t)$ is the Heaviside step function. The first term on the right-hand-side of Eq. (3) represents the diamagnetic London response, while the second term is the paramagnetic response from *both* the bulk and surface states. The above framework is general and the magnetic field in the slab is determined once the current-current correlation function is specified. In what follows we consider a clean system. Weak nonmagnetic disorder is not expected to modify the low-temperature response of the surface response (it is strongly irrelevant [49]) or of the fully gapped bulk.

Although the low-temperature, T^3-dependence of the penetration depth derived below depends only on the low-energy dispersion of the 2D Majorana surface fluid, here we consider a microscopic model for both the bulk and surface modes of the TSC in order to completely specify the problem. Solid state models analogous to ^{3}He provide a fertile playground to study topologically nontrivial superconductivity [2, 19, 24]. "Solid-state ^{3}He-A" would correspond to a Weyl superconductor, which has nodal Weyl points in the bulk that connect to a surface Majorana arc. In this work, we consider "solid-state ^{3}He-B" [24, 25], with isotropic p-wave pairing of spin-$1/2$ electrons, represented by the following Bogoliubov-de Gennes Hamiltonian

$$H = \frac{1}{2}\int_{\mathbf{k}}\chi^\dagger(\mathbf{k})\,\hat{h}(\mathbf{k})\,\chi(\mathbf{k}), \tag{5}$$

where

$$\hat{h}(\mathbf{k}) = \tilde{\varepsilon}_k\,\hat{\sigma}^3 + \Delta\,\hat{\mathbf{s}}\cdot\mathbf{k}\,\hat{\sigma}^2, \qquad \tilde{\varepsilon}_k = \frac{k^2}{2m} - \mu, \tag{6}$$

and where $\int_{\mathbf{k}} \equiv \int\frac{d^3\mathbf{k}}{(2\pi)^3}$, $\hat{\mathbf{s}}$ and $\hat{\boldsymbol{\sigma}}$ respectively denote Pauli matrices acting in the spin and particle-hole spaces, and $\chi(\mathbf{k}) \equiv \left[c(\mathbf{k}), \hat{s}^2\left[c^\dagger(-\mathbf{k})\right]^\mathsf{T}\right]$ is the four-component Balian-Werthammer spinor [50]. The latter satisfies the reality ("Majorana") condition $\chi^\dagger(\mathbf{k}) = i\chi^\mathsf{T}(-\mathbf{k})\hat{M}_\mathsf{P}$, where $\hat{M}_\mathsf{P} = \hat{s}^2\hat{\sigma}^2$ defines particle-hole symmetry for $\hat{h}(\mathbf{k})$. In Eq. (6), μ is the chemical potential and Δ is the

superconducting order parameter amplitude. For $\mu > 0$ the above Hamiltonian has winding number $\nu = 1$. The retarded paramagnetic current-current correlation function due to the bulk is

$$\tilde{\Pi}_{1,R}^{xx}(\Omega = 0, \mathbf{q} = 0) = -\frac{\beta}{6}\left(\frac{e}{m}\right)^2 \int_{\mathbf{k}} k^2 \operatorname{sech}^2\left(\frac{\beta E_k}{2}\right), (7)$$

where $E_k = \sqrt{\tilde{\varepsilon}_k^2 + \Delta^2 k^2}$ is the eigenenergy of $\hat{h}(\mathbf{k})$ and $\beta = T^{-1}$ is the inverse temperature. In the low-temperature limit, the bulk paramagnetic response is exponentially suppressed and the diamagnetic London response dominates. The London depth is given by $\lambda_L^{(0)} = \sqrt{mc^2/(4\pi e^2 n)}$, where n is the charge number density.

To consider the response from the surface, we replace $k_z \to -i\partial_z$ in $\hat{h}(\mathbf{k})$ [Eq. (6)] and solve for the Majorana surface states $\psi_{\mathbf{k}}^{\mathsf{s}}(z)$ with eigenenergies $\pm\Delta|\mathbf{k}|$. Here and in what follows, $\mathbf{k} = (k_x, k_y)$ specifies the momentum transverse to the interface. With hard wall boundary conditions at $z = 0$, we obtain surface wave functions of the form [51]

$$\psi_{\mathbf{k}}^{\mathsf{s}}(z) = \frac{e^{-z/l_{\mathsf{coh}}}}{\sqrt{N_{\mathbf{k}}^{\mathsf{s}}}} \sin\left(z\sqrt{\lambda_F^{-2} - l_{\mathsf{coh}}^{-2} - k^2}\right)|\psi_{\mathbf{k}}^0\rangle, \quad (8)$$

where N_k^{s} is a normalization constant and $|\psi_{\mathbf{k}}^0\rangle$ is a spin-momentum-locked spinor in (spin)⊗(particle-hole) space. The two length scales in Eq. (8) are the (reduced) Fermi wavelength $\lambda_F \equiv 1/\sqrt{2m\mu}$ and the coherence length $l_{\mathsf{coh}} \equiv 1/m\Delta$.

We can see how the magnetic field couples to the surface fluid by incorporating a vector potential $\mathbf{A}$ into Eq. (5), and then projecting onto the low-energy surface states. The result is

$$H_{\mathsf{s}} = \int_{\mathbf{r}}\left\{\frac{1}{2}\eta^\dagger(\mathbf{r})\left[-i\Delta(\hat{s}\wedge\boldsymbol{\nabla})\right]\eta(\mathbf{r}) - \frac{1}{c}\mathbf{A}\cdot\mathbf{J}\right\}, \quad (9)$$

where $\eta = \eta_s$ is the two-component surface Majorana fermion operator ($s \in \{\uparrow,\downarrow\}$), $\hat{s}\wedge\boldsymbol{\nabla} \equiv \hat{s}^1\partial_y - \hat{s}^2\partial_x$, and the surface paramagnetic current operator

$$\mathbf{J}(\mathbf{r}) = \frac{e}{4m}\eta^\dagger(\mathbf{r})i\overset{\leftrightarrow}{\boldsymbol{\nabla}}\eta(\mathbf{r}). \quad (10)$$

Here $\mathbf{r} = (x, y)$ and $\overset{\leftrightarrow}{\boldsymbol{\nabla}} \equiv \overset{\rightarrow}{\boldsymbol{\nabla}} - \overset{\leftarrow}{\boldsymbol{\nabla}}$. Eq. (9) assumes that the field $\mathbf{B}(z)$ and the vector potential $\mathbf{A}(z)$ (in London gauge) both reside in the (x, y) plane. Zeeman coupling to a nonzero component B_z would induce a Majorana mass, gapping out the surface fluid [1], but this is prevented by bulk Meissner screening. On the other hand, a very strong in-plane field $A_{x,y}$ could "overtilt" the surface Majorana cone, creating a surface Fermi pocket. The latter should be included in the diamagnetic current [52], but we exclude this situation here by restricting to linear response.

In the low-temperature limit, the paramagnetic current-current correlation function due to the surface state fluid evaluates to [51]

$$\tilde{\Pi}_{1,R,\mathsf{s},\mathsf{s}}^{xx}(0, 0, 0; q_z, -Q_z)$$
$$\simeq -\mathcal{C}\left(\frac{e}{m}\right)^2\frac{(k_B T)^3}{\Delta^4}\Theta(0, q_z)\Theta(0, -Q_z), \quad (11)$$

$\mathcal{C} \equiv [3^2\zeta(3)/(2^3\pi)]$, $\zeta(z)$ is the Riemann Zeta function, and where

$$\Theta(k, q_z) \equiv \int_0^\infty dz\, e^{-iq_z z}\,\psi_{\mathbf{k}}^{\mathsf{s}\dagger}(z)\,\psi_{\mathbf{k}}^{\mathsf{s}}(z) \quad (12)$$

is the Fourier transformed probability density of the surface states along the z-direction. Unlike the paramagnetic response from the bulk, the one from the surface [Eq. (11)] has a non-trivial T^3 power-law dependence at low temperature. Two factors of temperature arise from the form of the paramagnetic current operator (a derivative) in Eq. (10), while the third stems from the surface density of states of the Majorana fluid. One should also consider the surface-bulk cross terms when evaluating the paramagnetic current-current correlator appearing in Eq. (3). However, these cross terms exhibit higher-power temperature-dependence at low T, and are thus subleading [51]. We neglect these surface-bulk contributions in the following.

Results.—Taking only the diamagnetic and surface paramagnetic responses into account, which is valid at low temperature as discussed above, we can formally invert the integral equation Eq. (3) and solve for the vector potential (and hence the magnetic field) profile inside the slab. To leading order in temperature, the final result is [51]

$$B_y(z) = B_0\left\{e^{-z/\lambda_L^{(0)}} - \varrho(T)\left[\partial_z G(z)\right]G(0)\right\}, \quad (13)$$

where

$$\varrho(T) \equiv \left[2^4 3^3 \zeta(3)\pi\right]\left(\lambda_L^{(0)}\right)^6 l_{\mathsf{coh}}^{-1}\lambda_F^{-4}t^3 \quad (14)$$

is a temperature-dependent length, with $t \equiv k_B T/\Delta k_F$ being the dimensionless temperature. Here, Δk_F is the energy gap of the p-wave TSC. In Eq. (13), the function $G(z)$ is a temperature-independent, real-valued function encoding the convolution of the bulk and surface responses. It is a dimensionless function only of z and of the three lengths $\{\lambda_F, \lambda_L^{(0)}, l_{\mathsf{coh}}\}$. $G(z)$ emerges when we invert the integral equation and Fourier transform the quantities back to real space [51].

The first term in Eq. (13) describes the Meissner screening due to the diamagnetic London response, while the second term is the correction due to the Majorana surface fluid. The correction term depends on the length $\varrho(T)$ that encodes the T^3 dependence, while its spatial

dependence is captured by $G(z)$. The function $G(z)$ decays exponentially for large z; its spatial extent is governed by the maximum of $\{\lambda_L^{(0)}, l_{coh}/2\}$, assuming that λ_F is the shortest scale. This leads to different qualitative type I and II behaviors. Nevertheless, to characterize the overall spatial extent of the magnetic field, we can define the effective penetration depth of the system via [43]

$$\lambda(T) \equiv \frac{1}{B_0} \int_0^\infty dz\, B_y(z) = \lambda_L^{(0)} + \varrho(T) \left[G(0)\right]^2. \quad (15)$$

The second term in Eq. (15) is the change of the penetration depth due to the surface states. This term is always positive, meaning that the magnetic field can penetrate deeper into the slab for any $T > 0$, due to the surface Majorana fluid. It is instructive to roughly estimate the order of magnitude for such correction. For $Cu_x Bi_2 Se_3$, which is in the extreme type II regime, we substitute typical experimental data $l_{coh} \sim 10$ nm, $\lambda_F \sim 1$ nm, and $\lambda_L^{(0)} \sim 1$ μm [33, 53] to obtain $\delta\lambda(T) \sim 0.1\lambda_L^{(0)} t^3$.

The two physical quantities $B_y(z)$ and $\lambda(T)$ we focus on inherit the T^3 dependence from the surface current-current correlation function [Eq. (11)]. Similar power-law-dependence is observed in bulk nodal superconductors. In contrast to those systems, the model we considered is fully gapped in the bulk, and thus the Majorana surface states are responsible for the gapless excitations.

Although the exact expression for $G(z)$ is complicated [51], it takes relatively simple forms in the strong type-I and type-II limits. For a type-I TSC ($l_{coh} \gg \lambda_L^{(0)}$),

$$G_I(z) \simeq \frac{\lambda_F^2}{2\left(\lambda_L^{(0)}\right)^2 \left[4\left(\lambda_L^{(0)}\right)^2 + \lambda_F^2\right]} \Bigg\{ -\left(\lambda_L^{(0)}\right)^2 e^{-z/\lambda_L^{(0)}}$$
$$+ \left[2\left(\lambda_L^{(0)}\right)^2 + \lambda_F^2 \sin^2\left(\frac{z}{\lambda_F}\right)\right] e^{-2z/l_{coh}} \Bigg\}. \quad (16)$$

Since the coherence length sets the depth of the surface fluid [Eq. (8)], the latter allows a much deeper penetration of the field in the type-I limit than the bulk London depth. The slower decay is modulated by a Friedel oscillation. Representative field profiles are shown in Fig. 2(a).

For a type-II TSC ($l_{coh} \ll \lambda_L^{(0)}$),

$$G_{II}(z) \simeq \frac{\lambda_F^2 l_{coh}}{16\left(\lambda_L^{(0)}\right)^4} \left[\lambda_L^{(0)} e^{-z/\lambda_L^{(0)}} - l_{coh}\, e^{-2z/l_{coh}}\right]. \quad (17)$$

In this case the Friedel oscillating terms are subleading, and can be neglected. Note that the first term in Eq. (17) dominates the second. In this case the spatial field penetration is governed by the London depth, but the correction in Eqs. (13) and (17) effectively enhances the field amplitude. Representative field profiles are indicated in Fig. 2(b).

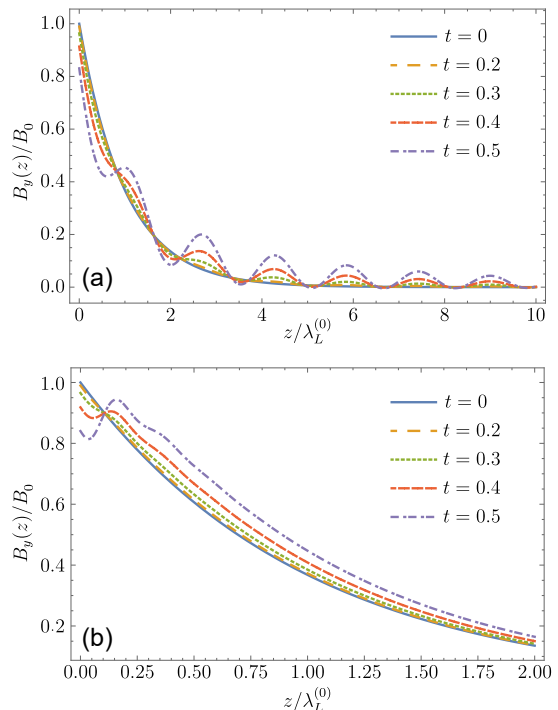*Conclusion.*—Our calculations suggest an alternative

FIG. 2: Plot of the magnetic field profile inside the topological superconductor (TSC) at different temperatures in the (a) type-I case with $\lambda_L^{(0)} = 1$, $l_{coh} = 10$, and $\lambda_F = 0.5$, and (b) type-II case with $\lambda_L^{(0)} = 30$, $l_{coh} = 8$, and $\lambda_F = 2$. Here $\lambda_F = 1/\sqrt{2m\mu}$ is the reduced Fermi wavelength, $l_{coh} = 1/m\Delta$ is the coherence length, and $\lambda_L^{(0)}$ is the London depth. The blue curves (at $t = 0$) represent the diamagnetic London response. The dimensionless temperature $t \equiv k_B T/\Delta k_F$, where Δk_F is the p-wave TSC energy gap. As temperature increases, the response from the surface becomes more pronounced. For type I (a), the correction from the surface exhibits Friedel oscillations and penetrates much deeper than the London depth. For type II (b), the strongest modulation due to the surface fluid appears close to the surface.

way to search for Majorana surface states in TSCs by measuring the change in the penetration depth $\delta\lambda(T)$. ARPES is often employed as the key tool to detect smoking gun signatures of topology in quantum materials. Unfortunately, TSC candidates typically have a small gap, making surface states difficult for ARPES to resolve [28]. A necessary, but not sufficient condition for the existence of a gapless Majorana surface fluid can be the signature power-law dependence $\delta\lambda(T) \sim T^3$. This can be probed by means of tunnel-diode oscillator techniques [39–42]. While $\delta\lambda(T)$ is exponentially suppressed in conventional, topologically trivial superconductors, a power-law $\delta\lambda(T) \sim T^\alpha$ is also expected in superconductors with nodal bulk excitations, where α depends on whether the nodes are points or lines [43, 54]. For example, a power-law with $\alpha = 1$ has been observed in high-T_c d-wave superconductors [46].

One way to distinguish the origin of a penetration-

depth power law (Majorana surface states versus bulk nodes) is via a specific-heat measurement versus temperature. The specific heat due to the 2D surface of a fully gapped 3D TSC is negligible. In addition to $\delta\lambda(T) \sim T^\alpha$, a TSC with a fully gapped bulk (nodal superconductor) should therefore demonstrate exponential suppression (power-law dependence) in specific heat [54].

The superconducting doped topological insulators $(Cu,Nb)_xBi_2Se_3$ [39, 40, 53] and the half-Heusler compound YPtBi [41, 55] are all strongly type II. Power-law dependence of $\lambda(T)$ was observed in $Nb_xBi_2Se_3$ [39, 40], YPtBi [41], and in YPdBi and TbPdBi [42]. It would be interesting to assess whether any of these could be attributed to the presence of Majorana surface states. In particular, it is worthwhile to note that while specific-heat measurements suggest a fully gapped bulk in $Cu_xBi_2Se_3$ and $Ni_xBi_2Se_3$[31, 32], penetration depth data for $Ni_xBi_2Se_3$ shows a power-law dependence [39, 40]. In the case of half-Heusler compounds such as YPtBi, it has been suggested that optical-phonon-mediated pairing could favor a fully gapped TSC state with winding number $\nu = 3$ [56], and this should induce novel, cubic-dispersing Majorana surface fermions [45, 57]. In this case, we would expect a very slow $\delta\lambda(T) \sim T^{1/3}$ dependence for a clean, cubically-dispersing Majorana surface fluid. However, the results due to surface states with $\nu \geq 3$ might be strongly modified by quenched disorder [45, 58].

In this Letter, calculations were performed for a clean system. On one hand, low-energy Majorana surface states with winding number $\nu = 1$ are not affected by non-magnetic impurities [49, 58]; weak nonmagnetic disorder should therefore not alter the cubic power law $\delta\lambda(T) \sim T^3$ predicted here as $T \to 0$. The power can possibly be modified by strong (resonant) impurity scattering [46]. On the other hand, magnetic impurities can strongly perturb the surface states, and even gap them out. Moreover, magnetic impurities may independently induce power-law dependence in $\delta\lambda(T)$, by altering the magnetic permeability [46, 47].

[1] X. L. Qi and S. C. Zhang, Topological insulators and superconductors, Rev. Mod. Phys. **83**, 1057 (2011).

[2] M. Sato and Y. Ando, Topological superconductors: a review, Rep. Prog. Phys. **80**, 076501 (2017).

[3] J. Alicea, New directions in the pursuit of Majorana fermions in solid state systems, Rep. Prog. Phys. **75**, 076501 (2012).

[4] F. Wilczek, Majorana returns, Nat. Phys. **5**, 614 (2009).

[5] V. Mourik, K. Zuo, S. M. Frolov, S. R. Plissard, E. P. A. M. Bakkers, and L. P. Kouwenhoven, Signatures of Majorana Fermions in Hybrid Superconductor-Semiconductor Nanowire Devices, Science **336**, 1003 (2012).

[6] A. Das, Y. Ronen, Y. Most, Y. Oreg, M. Heiblum, and H. Shtrikman, Zero-bias peaks and splitting in an Al-InAs nanowire topological superconductor as a signature of Majorana fermions, Nat. Phys. **8**, 887 (2012).

[7] A. D. K. Finck, D. J. Van Harlingen, P. K. Mohseni, K. Jung, and X. Li, Anomalous Modulation of a Zero-Bias Peak in a Hybrid Nanowire-Superconductor Device, Phys. Rev. Lett. **110**, 126406 (2013).

[8] E. J. H. Lee, X. Jiang, R. Aguado, G. Katsaros, C. M. Lieber, and S. De Franceschi, Zero-Bias Anomaly in a Nanowire Quantum Dot Coupled to Superconductors, Phys. Rev. Lett. **109**, 186802 (2012).

[9] S. Cho, R. Zhong, J. A. Schneeloch, G. Gu, and N. Mason, Kondo-like zero-bias conductance anomaly in a three-dimensional topological insulator nanowire, Sci. Rep. **6**, 21767 (2016).

[10] L. Fu and C. L. Kane, Josephson current and noise at a superconductor/quantum-spin-Hall-insulator/superconductor junction, Phys. Rev. B **79**, 161408(R) (2009).

[11] L. Fu and C. L. Kane, Superconducting Proximity Effect and Majorana Fermions at the Surface of a Topological Insulator, Phys. Rev. Lett. **100**, 096407 (2008).

[12] E. Taylor, A. J. Berlinsky, and C. Kallin, Locally gauge-invariant spin response of ^{3}He$-$B films with Majorana surface states, Phys. Rev. B **91**, 134505 (2015).

[13] K. H. A. Villegas, V. M. Kovalev, F. V. Kusmartsev, and I. G. Savenko, Shedding light on topological superconductors, Phys. Rev. B **98**, 064502 (2018).

[14] A. P. Mackenzie and Y. Maeno, The superconductivity of Sr_2RuO_4 and the physics of spin-triplet pairing, Rev. Mod. Phys. **75**, 657 (2003).

[15] C. Kallin, Chiral p-wave order in Sr_2RuO_4, Rep. Prog. Phys. **75**, 042501 (2012).

[16] C. Kallin, Chiral superconductors, Rep. Prog. Phys. **79**, 054502 (2016).

[17] A. P. Schnyder, S. Ryu, A. Furusaki, and A. W. W. Ludwig, Classification of topological insulators and superconductors in three spatial dimensions, Phys. Rev. B **78**, 195125 (2008).

[18] R. Roy, Topological superfluids with time reversal symmetry, arXiv:0803.2868.

[19] G. E. Volovik, Topological Invariant for Superfluid ^{3}He-B and Quantum Phase Transitions, JETP Lett. **90**, 587 (2009).

[20] X.-L. Qi, T. L. Hughes, S. Raghu, and S.-C. Zhang, Time-Reversal-Invariant Topological Superconductors and Superfluids in Two and Three Dimensions, Phys. Rev. Lett. **102**, 187001 (2009).

[21] M. Sato, Topological properties of spin-triplet superconductors and Fermi surface topology in the normal state, Phys. Rev. B **79**, 214526 (2009).

[22] M. Sato, Topological odd-parity superconductors, Phys. Rev. B **81**, 220504(R) (2010).

[23] T. Mizushima, Y. Tsutsumi, T. Kawakami, M. Sato, M. Ichioka, and K. Machida, Symmetry Protected Topological Superfluids and Superconductors –From the Basics to ^{3}He–, J. Phys. Soc. Jpn. **85**, 022001 (2016).

[24] G. E. Volovik, *The Universe in a Helium Droplet* (Oxford University Press, Oxford, 2003).

[25] B. A. Bernevig and T. L. Hughes, *Topological Insulators and Topological Superconductors* (Princeton University Press, Princeton, New Jersey, 2013).

[26] L. Fu and E. Berg, Odd-Parity Topological Superconductors: Theory and Application to $Cu_x Bi_2 Se_3$, Phys. Rev. Lett. **105**, 097001 (2010).

[27] L. Fu, Odd-parity topological superconductor with nematic order: Application to $Cu_x Bi_2 Se_3$, Phys. Rev. B **90**, 100509(R) (2014).

[28] L. A. Wray, S.-Y. Xu, Y. Xia, Y. S. Hor, D. Qian, A. V. Fedorov, H. Lin, A. Bansil, R. J. Cava, and M. Z. Hasan, Observation of topological order in a superconducting doped topological insulator, Nat. Phys. **6**, 855 (2010).

[29] P. Hosur, X. Dai, Z. Fang, and X.-L. Qi, Time-reversal-invariant topological superconductivity in doped Weyl semimetals, Phys. Rev. B **90**, 045130 (2014).

[30] K. Matano, M. Kriener, K. Segawa, Y. Ando, and G.-q. Zheng, Spin-rotation symmetry breaking in the superconducting state of $Cu_x Bi_2 Se_3$, Nat. Phys. **12**, 852 (2016).

[31] S. Yonezawa, K. Tajiri, S. Nakata, Y. Nagai, Z. Wang, K. Segawa, Y. Ando, and Y. Maeno, Thermodynamic evidence for nematic superconductivity in $Cu_x Bi_2 Se_3$, Nat. Phys. **13**, 123 (2017).

[32] T. Asaba, B. J. Lawson, C. Tinsman, L. Chen, P. Corbae, G. Li, Y. Qiu, Y. S. Hor, L. Fu, and L. Li, Rotational Symmetry Breaking in a Trigonal Superconductor Nb-doped $Bi_2 Se_3$, Phys. Rev. X **7**, 011009 (2017).

[33] R. Tao, Y.-J. Yan, X. Liu, Z.-W. Wang, Y. Ando, Q.-H. Wang, T. Zhang, and D.-L. Feng, Direct Visualization of the Nematic Superconductivity in $Cu_x Bi_2 Se_3$, Phys. Rev. X **8**, 041024 (2018).

[34] M. Chen, X. Chen, H. Yang, Z. Du, and H.-H. Wen, Superconductivity with twofold symmetry in $Bi_2 Te_3 / FeTe_{0.55} Se_{0.45}$ heterostructures, Sci. Adv. **4**, eaat1084 (2018).

[35] S. Sasaki, M. Kriener, K. Segawa, K. Yada, Y. Tanaka, M. Sato, and Y. Ando, Topological Superconductivity in $Cu_x Bi_2 Se_3$, Phys. Rev. Lett. **107**, 217001 (2011).

[36] H. Peng, D. De, B. Lv, F. Wei, and C.-W. Chu, Absence of zero-energy surface bound states in $Cu_x Bi_2 Se_3$ studied via Andreev reflection spectroscopy, Phys. Rev. B **88**, 024515 (2013).

[37] N. Levy, T. Zhang, J. Ha, F. Sharifi, A. A. Talin, Y. Kuk, and J. A. Stroscio, Experimental Evidence for s-Wave Pairing Symmetry in Superconducting $Cu_x Bi_2 Se_3$ Single Crystals Using a Scanning Tunneling Microscope, Phys. Rev. Lett. **110**, 117001 (2013).

[38] A. Kolapo, T. Li, P. Hosur, and J. H. Miller, Transport evidence for three dimensional topological superconductivity in doped β-$PdBi_2$, Sci. Rep., **9**, 12504 (2019).

[39] M. P. Smylie, H. Claus, U. Welp, W.-K. Kwok, Y. Qiu, Y. S. Hor, and A. Snezhko, Evidence of nodes in the order parameter of the superconducting doped topological insulator $Nb_x Bi_2 Se_3$ via penetration depth measurements, Phys. Rev. B **94**, 180510(R) (2016)

[40] M. P. Smylie, K. Willa, H. Claus, A. Snezhko, I. Martin, W.-K. Kwok, Y. Qiu, Y. S. Hor, E. Bokari, P. Niraula, A. Kayani, V. Mishra, and U. Welp, Robust odd-parity superconductivity in the doped topological insulator $Nb_x Bi_2 Se_3$, Phys. Rev. B **96**, 115145 (2017).

[41] H. Kim, K. Wang, Y. Nakajima, R. Hu, S. Ziemak, P. Syers, L. Wang, H. Hodovanets, J. D. Denlinger, P. M. R. Brydon, D. F. Agterberg, M. A. Tanatar, R. Prozorov, and J. Paglione, Beyond triplet: Unconventional superconductivity in a spin-3/2 topological semimetal, Sci. Adv. **4**, eaao4513 (2018).

[42] S. M. A. Radmanesh, C. Martin, Y. Zhu, X. Yin, H. Xiao, Z. Q. Mao, and L. Spinu, Evidence for unconventional superconductivity in half-Heusler YPdBi and TbPdBi compounds revealed by London penetration depth measurements, Phys. Rev. B **98**, 241111(R) (2018).

[43] M. Tinkham, *Introduction to Superconductivity*, 2nd ed. (Dover Publications, Mineola, New York, 2004).

[44] P. M. R. Brydon, L. Wang, M. Weinert, and D. F. Agterberg, Pairing of $j = 3/2$ Fermions in Half-Heusler Superconductors, Phys. Rev. Lett. **116**, 177001 (2016)

[45] B. Roy, S. A. A. Ghorashi, M. S. Foster, and A. H. Nevidomskyy, Topological superconductivity of spin-3/2 carriers in a three-dimensional doped Luttinger semimetal, Phys. Rev. B **99**, 054505 (2019).

[46] R. Prozorov and R. W. Giannetta, Magnetic penetration depth in unconventional superconductors, Supercond. Sci. Technol. **19**, R41 (2006).

[47] J. R. Cooper, Power-law dependence of the *ab*-plane penetration depth in $Nd_{1.85} Ce_{0.15} CuO_{4-y}$, Phys. Rev. B **54**, R3753(R) (1996).

[48] H. Wu and J. A. Sauls, Majorana excitations, spin and mass currents on the surface of topological superfluid ^{3}He-B, Phys. Rev. B **88**, 184506 (2013).

[49] S. A. A. Ghorashi and M. S. Foster, Criticality Across the Energy Spectrum from Random, Artificial Gravitational Lensing in Two-Dimensional Dirac Superconductors, arXiv:1903.11086.

[50] R. Balian and N. R. Werthammer, Superconductivity with Pairs in a Relative p Wave, Phys. Rev. **131**, 1553 (1963).

[51] See Supplemental Material at (link) for the derivation of Eqs. (7), (8), (11), and (13), and the explicit expression for $G(z)$, which takes the limiting forms shown in Eqs. (16) and (17) and which determines the coefficient in Eq. (15).

[52] L. Chirolli and F. Guinea, Signatures of surface Majorana modes in the magnetic response of topological superconductors, Phys. Rev. B **99**, 014506 (2019).

[53] M. Kriener, K. Segawa, S. Sasaki, and Y. Ando, Anomalous suppression of the superfluid density in the $Cu_x Bi_2 Se_3$ superconductor upon progressive Cu intercalation, Phys. Rev. B **86**, 180505(R) (2012).

[54] M. Sigrist and K. Ueda, Phenomenological theory of unconventional superconductivity, Rev. Mod. Phys. **63**, 239 (1991).

[55] T. V. Bay, T. Naka, Y. K. Huang, and A. de Visser, Superconductivity in noncentrosymmetric YPtBi under pressure, Phys. Rev. B **86**, 064515 (2012).

[56] L. Savary, J. Ruhman, J. W. F. Venderbos, L. Fu, and P. A. Lee, Superconductivity in three-dimensional

spin-orbit coupled semimetals, Phys. Rev. B **96**, 214514 (2017).

[57] C. Fang, B. A. Bernevig, and M. J. Gilbert, Tri-Dirac surface modes in topological superconductors, Phys. Rev. B **91**, 165421 (2015).

[58] M. S. Foster, H.-Y. Xie, and Y.-Z. Chou, Topological protection, disorder, and interactions: Survival at the surface of 3D topological superconductors, Phys. Rev. B **89**, 155140 (2014).